

Determination of the Spiral Pattern Speed in the Galaxy from Three Samples of Stars

V. V. Bobylev¹, A. T. Bajkova

Pulkovo Astronomical Observatory, Russian Academy of Sciences, St. Petersburg, 196140 Russia

We invoke the estimates of the amplitudes of the velocity perturbations f_R and f_θ caused by the influence of a spiral density wave that have been obtained by us previously from three stellar samples. These include Galactic masers with measured VLBI trigonometric parallaxes and proper motions, OB2 stars, and Cepheids. From these data we have obtained new estimates of the spiral pattern speed in the Galaxy Ω_p : 24.61 ± 2.06 , 24.71 ± 1.29 and 25.98 ± 1.37 km s⁻¹ kpc⁻¹ from the samples of masers, OB2 stars, and Cepheids, respectively. The corotation radii for these three samples R_{cor}/R_0 are 1.16 ± 0.09 , 1.15 ± 0.06 and 1.09 ± 0.06 , suggesting that the corotation circle is located between the Sun and the Perseus arm segment.

INTRODUCTION

Studying the spiral structure of the Galaxy is of great interest. The spiral structure tracers, for example, hydrogen clouds, OB stars, or Cepheids, are well known. Various methods of determining such parameters as the spiral pattern pitch angle i , the number of spiral arms m , the spiral pattern speed Ω_p , and the position of the corotation radius R_{cor} have been proposed. However, there is no complete agreement between the results of various authors.

Beginning with the pioneering studies of Lin and Shu (1964), Lin et al. (1969), and Yuan (1969) devoted to the application of the linear spiral density wave theory to the analysis of real data, a huge number of scientific publications are devoted to this problem. For example, the studies of Marochnik et al. (1972), Crézé and Mennessier (1973), Byl and Ovenden (1978), Mishurov et al. (1979), Loktin and Matkin (1992), Mishurov et al. (1997), Amaral and Lépine (1997), Rastorguev et al. (2001), Fernández et al. (2001), Dias and Lépine (2005), Junqueira et al. (2015), Dambis et al. (2015), Dias et al. (2019), Castro-Ginard et al. (2021), and Joshi and Malhotra (2023) can be noted.

The two-armed model of a spiral pattern with $m = 2$ and $i \sim -6^\circ$ has often been used previously. In recent years, there has been more inclination toward the four-armed model with $m = 4$ and $i \sim -12^\circ$. A large body of evidence precisely for the four-armed global spiral pattern was collected in the reviews by Vallée (1995, 2002, 2008, 2017a), although the case in point is a global spiral pattern with a constant pitch angle, the same for all arms. In recent years, however, the four-armed model with a sector structure of arms (Reid et al.

¹vbobylev@gaoran.ru

2014, 2019), which is substantiated by the analysis of masers with highly accurate VLBI measurements of their trigonometric parallaxes, has gained in popularity.

Accurate values of the spiral pattern speed and the corotation radius are of great interest. However, the present-day estimates of these parameters lie in a wide range. For example, it was concluded in the review by Gerhard (2011) that the spiral pattern speed is slightly smaller than the rotation rate of the Galaxy at the solar distance R_0 . This means that the corotation radius is slightly farther than R_0 . According to tracers with ages of $10^7 - 10^8$ yr, the average Ω_p is $25.2 \text{ km s}^{-1} \text{ kpc}^{-1}$. However, the studies devoted to the distribution of stellar velocities in the solar neighborhood give a wider range of Ω_p : $17-28 \text{ km s}^{-1} \text{ kpc}^{-1}$. Jacques Vallée regularly reviews the parameters of the Galactic spiral structure. In one of his latest studies he found (Vallée 2017b) that, on average, Ω_p is close to $23 \pm 2 \text{ km s}^{-1} \text{ kpc}^{-1}$.

The position of the corotation radius is of great and, occasionally, critical importance in modeling some processes. The point is that in a rotating reference frame the density wave moves from corotation to the Galactic center and from corotation into the outer Galaxy. As shown by Acharova et al. (2010), the combined effect of the corotation resonance and turbulent diffusion is responsible for the formation of a bimodal radial distribution of iron and oxygen in the Galactic disk. Another example: open star clusters in the corotation region, while undergoing small radial oscillations, are scattered upon disruption over a huge disk space (Mishurov and Acharova 2011).

In a number of our papers (Bobylev and Bajkova 2022a, 2022b, 2022d) we found the amplitudes of the velocity perturbations f_R and f_θ caused by the influence of a spiral density wave and estimated the angular velocity of Galactic rotation. These parameters were found from three samples: from Galactic masers with measured VLBI trigonometric parallaxes and proper motions, OB2 stars, and Cepheids. To determine f_R and f_θ , we applied a spectral analysis of the residual stellar velocities. The goal of this paper is to estimate the spiral pattern speed Ω_p in the Galaxy and the position of the corotation radius R_{cor} based on these data.

METHOD

The position of a star in a logarithmic spiral wave can be written as

$$R = R_0 e^{(\theta - \theta_0) \tan i}, \quad (1)$$

where R is the Galactocentric distance of the star; R_0 is the Galactocentric distance of the Sun; θ is the position angle of the star: $\tan \theta = y/(R_0 - x)$, where x, y are the heliocentric Galactic rectangular coordinates of the star, with the x axis being directed from the Sun to the Galactic center and the direction of the y axis coinciding with the direction of Galactic rotation; θ_0 is some arbitrarily chosen initial angle; i is the pitch angle of the spiral pattern ($i < 0$ for a winding spiral). After taking the logarithm of the left and right parts, Eq. (1) can be rewritten as

$$\ln\left(\frac{R}{R_0}\right) = \theta \tan i + \text{const}, \quad (2)$$

According to the spiral density wave theory of Lin and Shu (1964), Eq. (2) appears as (Yuan 1969)

$$\ln\left(\frac{R}{R_0}\right) = \tan i \left(\theta + \frac{\chi - \chi_0}{m} - \Omega_p t \right), \quad (3)$$

where χ is the radial phase of the wave, χ_0 is the position of the Sun in the wave, Ω_p is the spiral pattern speed, t is the time, and m is the number of spiral arms.

The relation (Rohlfis 1977) that follows from the linear density wave theory of Lin and Shu (1964) underlies the approach that we apply in this paper:

$$\chi = m[\Omega_p - \Omega(R)]t + \ln\left(\frac{R}{R_0}\right) \cot i = \varkappa \nu t + \ln\left(\frac{R}{R_0}\right) \cot i, \quad (4)$$

where $\Omega = \Omega(R)$ is the angular velocity of Galactic rotation, $\varkappa^2 = 4\Omega^2 \left(1 + \frac{R}{2\Omega} \frac{d\Omega}{dR}\right)$ is the epicyclic frequency ($\varkappa > 0$), $\nu = m(\Omega_p - \Omega)/\varkappa$ is the frequency with which a test particle encounters the passing spiral perturbation.

The influence of a spiral density wave on the rectangular heliocentric space velocities of a star U and V is periodic and, therefore, is represented as follows (Cr ez e and Mennessier 1973; Mishurov et al. 1979):

$$\begin{aligned} U &= f_R \cos \chi, \\ V &= f_\theta \sin \chi, \end{aligned} \quad (5)$$

where the velocity perturbation amplitudes f_R and f_θ can be found from observations, for example, by solving the kinematic equations or through a spectral analysis of the residual (freed from the peculiar solar motion and the Galactic rotation) stellar velocities. Note that both velocity perturbations f_R and f_θ that we found based on our spectral analysis are positive.

On the other hand, f_R and f_θ have the following form:

$$f_R = \frac{kA}{\varkappa} \frac{\nu}{1 - \nu^2} \mathfrak{S}_\nu^{(1)}(x), \quad f_\theta = -\frac{kA}{2\Omega} \frac{1}{1 - \nu^2} \mathfrak{S}_\nu^{(2)}(x), \quad (6)$$

where A is the amplitude of the spiral wave potential, $k = m \cot(i)/R$ is the radial wave number, $\mathfrak{S}_\nu^{(1)}(x)$ and $\mathfrak{S}_\nu^{(2)}(x)$ are the reduction factors,

$$\mathfrak{S}_\nu^{(1)}(x) = \frac{1 - \nu^2}{x} \left[1 - \frac{\nu\pi}{\sin(\nu\pi)} \frac{1}{2\pi} \int_{-\pi}^{+\pi} e^{-x(1+\cos(s))} \cos(\nu s) ds \right], \quad (7)$$

$$\mathfrak{S}_\nu^{(2)}(x) = (\nu^2 - 1) \frac{\nu\pi}{\sin(\nu\pi)} \frac{\partial}{\partial x} \left[\frac{1}{2\pi} \int_{-\pi}^{+\pi} e^{-x(1+\cos(s))} \cos(\nu s) ds \right], \quad (8)$$

which are functions of the coordinate $x = k^2 \sigma_R^2 / \varkappa^2$, where σ_R is the root-mean-square (rms) stellar radial velocity dispersion. Relations (6)–(9) allows Ω_p to be determined after substituting the parameters ($f_R, f_\theta, \Omega_0, \Omega'_0, \sigma_R$) derived from observations.

We estimate the amplitude of the spiral wave potential based on the well-known relation (Fern andez et al. 2008)

$$A = \frac{(R_0 \Omega_0)^2 f_{r0} \tan i}{m}, \quad (9)$$

where we take the ratio of the radial component of the gravitational force corresponding to the spiral arms to the total gravitational force of the Galaxy, f_{r0} , to be 0.04 ± 0.01 (Bobylev and Bajkova 2012). In this paper we use the four-armed Galactic spiral pattern ($m = 4$) with the pitch angle $i = -12.5^\circ$. We take R_0 to be 8.1 ± 0.1 kpc, according to the review by Bobylev and Bajkova (2021), where it was deduced as a weighted mean of a large number of present-day individual estimates.

Given the ratio $\mathfrak{S}_\nu^{(2)}/\mathfrak{S}_\nu^{(1)}$, the value of Ω_p found can be checked according to the expression derived from (6) and (7) for $R = R_0$ and $\Omega = \Omega_0$:

$$\Omega_p - \Omega_0 = -\frac{\mathfrak{S}_\nu^{(2)}}{\mathfrak{S}_\nu^{(1)}} \frac{f_R}{f_\theta} \frac{2\Omega_0}{m} \left(1 + \frac{R_0\Omega'_0}{2\Omega_0}\right). \quad (10)$$

RESULTS

Table 1 summarizes the results of our determination of the spiral pattern speed Ω_p and the corotation radius R_{cor} from three samples of young objects. These include masers, OB2 stars, and Cepheids.

We calculated the corotation radius based on the relation derived by equating the linear rotation velocity of the Galaxy and the rotation velocity of the spiral pattern found:

$$R_{\text{cor}} = R_0 + (\Omega_p - \Omega_0)/\Omega'_0. \quad (11)$$

Masers

In Bobylev and Bajkova (2022b) we analyzed a sample of masers and radio stars with measured VLBI trigonometric parallaxes; only objects with parallax measurement errors less than 10% were considered.

The catalogues by Reid et al. (2019) and Hirota et al. (2020) served as the main sources of data. Data on 199 masers were included in the list by Reid et al. (2019). The VLBI observations were carried out at several radio frequencies within the BeSSeL (the Bar and Spiral Structure Legacy Survey ¹) project. Hirota et al. (2020) presented a catalog of 99 maser sources observed exclusively at 22 GHz within the VERA (VLBI Exploration of Radio Astrometry ²) program.

The distribution of the masers and radio stars used in projection onto the Galactic XY plane is given in Fig. 1. The coordinate system in which the X axis is directed from the Galactic center to the Sun and the direction of the Y axis coincides with the direction of Galactic rotation is used in this figure. The four-armed spiral pattern with the pitch angle $i = -13^\circ$ from Bobylev and Bajkova (2014) is given; here, it was constructed with $R_0 = 8.1$ kpc, the Roman numerals number the following four spiral arms: Scutum (I), Carina-Sagittarius (II), Perseus (III), and the Outer Arm (IV).

The Local Arm (~ 70 sources) is well represented in Fig. 1. Nevertheless, a concentration of stars to the Perseus, Carina-Sagittarius, and Scutum arm segments is seen.

The angular velocity of Galactic rotation and its two derivatives were estimated using 150 masers from the Galactic region $R > 4$ kpc, while the velocity perturbations f_R and f_θ were estimated by applying a spectral analysis of the residual velocities of masers within 5 kpc of the Sun. Based on this sample of masers, we calculated the rms radial velocity dispersion to be $\sigma_R = 12$ km s⁻¹.

OB2 stars

The angular velocity of Galactic rotation and its derivatives were estimated in Bobylev and Bajkova (2022a) by analyzing the proper motions of 9750 OB2 stars. The sample of OB2

¹<http://bessel.vlbi-astrometry.org>

²<http://veraserver.mtk.nao.ac.jp>

Table 1: Estimates of the spiral pattern parameters Ω_p and R_{cor}

Parameters	Masers	OB2 stars	Cepheids
N_\star	150	1812	363
Ω_0 , km s ⁻¹ kpc ⁻¹	30.18 ± 0.38	29.71 ± 0.06	28.87 ± 0.23
Ω'_0 , km s ⁻¹ kpc ⁻²	-4.368 ± 0.077	-4.014 ± 0.018	-3.894 ± 0.063
f_R , km s ⁻¹	8.1 ± 1.4	4.8 ± 0.7	5.5 ± 2.0
f_θ , km s ⁻¹	6.1 ± 1.7	4.1 ± 0.9	7.1 ± 2.0
σ_R , km s ⁻¹	12	13.4	15
Source	(1)	(2)	(3)
Ω_p , km s ⁻¹ kpc ⁻¹	24.61 ± 2.06	24.71 ± 1.29	25.98 ± 1.37
R_{cor} , kpc	9.37 ± 0.78	9.34 ± 0.49	8.84 ± 0.47
R_{cor}/R_0	1.16 ± 0.09	1.15 ± 0.06	1.09 ± 0.06
$\mathfrak{S}_\nu^{(2)}/\mathfrak{S}_\nu^{(1)}$	0.672	0.635	0.569

N_\star is the number of stars used; (1) Bobylev and Bajkova (2022b); (2) Bobylev and Bajkova (2022a, 2022c); (3) Bobylev and Bajkova (2022d).

stars from Xu et al. (2021) with proper motions and trigonometric parallaxes from the Gaia EDR3 catalogue was used for this purpose.

Based on this sample, we also found the principal axes of the ellipsoid of residual velocity dispersions for OB2 stars, $\sigma_1, \sigma_2, \sigma_3 = (11.79, 9.66, 7.21) \pm (0.06, 0.05, 0.04)$ km s⁻¹, and showed that the first axis of this ellipsoid deviates from the direction to the Galactic center by a small angle of about 12°. Thus, σ_1 can be used as the radial velocity dispersion σ_R in relations (6)–(9).

The kinematics of the total space velocities of OB2 stars was studied in Bobylev and Bajkova (2022c). These include 1812 stars with measured line-of-sight velocities, proper motions, and trigonometric parallaxes. The distribution of these OB2 stars in projection onto the Galactic XY plane is given in Fig. 2. We determined the velocity perturbation amplitudes f_R and f_θ from them by applying a spectral analysis of the residual velocities. As can be seen from the figure, the Local Arm as well as the Carina-Sagittarius and Perseus arms are well represented.

A direct calculation of the radial velocity dispersion based on this sample of OB2 stars gave $\sigma_R = 13.4$ km s⁻¹. Thus, the line-of-sight velocity errors increased σ_R compared to $\sigma_1 = 11.79$ km s⁻¹ obtained by analyzing only the stellar proper motions.

Cepheids

The angular velocity of Galactic rotation and its derivatives were estimated from a sample of Cepheids in Bobylev and Bajkova (2022d). A sample of 363 Cepheids younger than 120 Myr located no farther than 5 kpc from the Sun was used for this purpose. Their average age is 85 Myr. We took the proper motions of these stars from the Gaia EDR3 catalogue.

The paper by Skowron et al. (2019), where the distances, ages, pulsation periods, and photometric data are given for 2431 classical Cepheids, served as a basis for studying the sample of Cepheids. The observations of these variable stars were performed within the OGLE (Optical Gravitational Lensing Experiment) program (Udalski et al. 2015). The distances to the Cepheids were calculated based on the calibration period–luminosity rela-

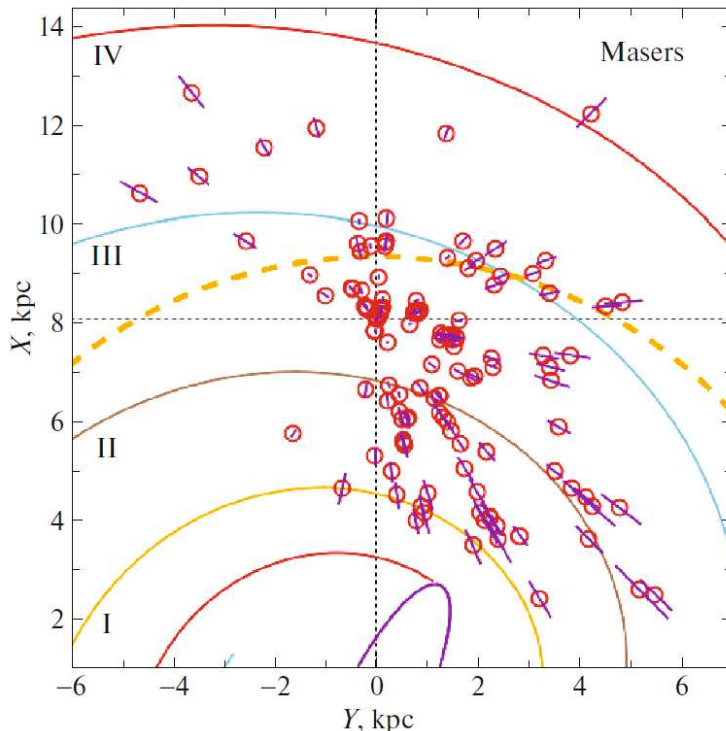


Figure 1: Distribution of 150 masers and radio stars with trigonometric parallax errors less than 10% in projection onto the Galactic XY plane, the distance errors bars are given for each star, the four-armed spiral pattern with the pitch angle $i = -13^\circ$ is shown, the central Galactic bar is marked, the thick dashed line indicates the corotation circle found.

tions found by Wang et al. (2018) from the mid-infrared light curves of Cepheids for eight bands. These include four bands of the WISE (Wide-field Infrared Survey Explorer, Chen et al. 2018) catalogue, W1–W4: [3.35], [4.60], [11.56], and [22.09] μm , and four bands of GLIMPSE (Spitzer Galactic Legacy Infrared Mid-Plane Survey Extraordinaire, Benjamin et al. 2003): [3.6], [4.5], [5.8], and [8.0] μm . The extinction A_{K_s} was calculated from extinction maps for each star in the catalogue by Skowron et al. (2019). According to these authors, the error in the distance to the Cepheids in their catalogue is $\sim 5\%$. Skowron et al. (2019) estimated the ages using the technique of Anderson et al. (2016) by taking into account the spin period of the stars and the metallicity index.

The distribution of Cepheids younger than 120 Myr in projection onto the Galactic XY plane is given in Fig. 2. The dark dots in this figure mark 363 Cepheids located no farther than 5 kpc from the Sun, where the sample satisfies the completeness condition. Only the Carina-Sagittarius arm segment is well represented in the figure. From these 363 Cepheids we determined the velocity perturbation amplitudes f_R and f_θ based on a spectral analysis of the residual stellar velocities. The value of $\sigma_R = 15 \text{ km s}^{-1}$ for these stars can be estimated from the error per unit weight obtained when solving the kinematic equations in Bobylev and Bajkova (2022d). A direct calculation based on 363 Cepheids with measured line-of-sight velocities gave a close value, $\sigma_R = 14.9 \text{ km s}^{-1}$.

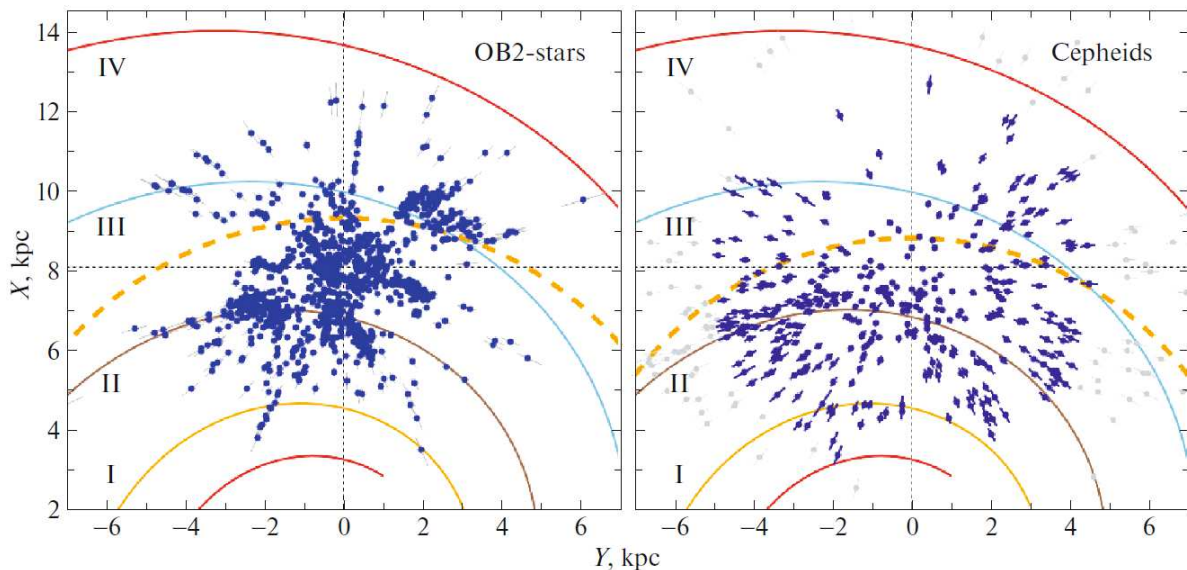


Figure 2: Distribution of OB2 stars (left) and Cepheids (right) in projection onto the Galactic XY plane, the error bars that correspond to the declared distance errors in the corresponding catalogue are given, the four-armed spiral pattern with the pitch angle $i = -13^\circ$ is shown, the thick dashed lines indicate the corresponding corotation circles.

DISCUSSION

Table 2 gives the estimates of Ω_p by various methods. These results were obtained mostly from such young objects as OB stars, open star clusters (OSCs), and Cepheids.

As is well known, the first estimates of Ω_p found by Lin et al. (1969) and Yuan (1969) provoked a debate (Marochnik et al. 1972) about the choice of the most probable value, 13 or 23 km s^{-1} . However, choosing the true value of Ω_p is a no less acute problem even now. A discussion of this problem can be found, for example, in Palouš et al. (1977), Palouš (1980), Marochnik and Suchkov (1981), Pichardo et al. (2003), or Martos et al. (2004).

Surprisingly, but there are estimates with small $\Omega_p = 12 \text{ km s}^{-1}$ obtained by Eilers et al. (2020) and Vallée (2021) from present-day data even now. However, we did not include these estimates in the table by deeming them exotic.

In the table we did not include the results of simulations (for example, Quillen and Minchev 2005; Chakrabarty 2007; Michtchenko et al. 2018) obtained with prespecified Ω_p by deeming these estimates indirect. The studies where the authors either did not decide on the mean value of Ω_p (Griv et al. 2017) or found Ω_p separately from a particular spiral arm segment (Naoz and Shaviv 2007) were not included either. However, it can be already seen that the present-day results lie in a very wide range of Ω_p : 18–32 km s^{-1} .

Direct Method

A simple relation follows from Eq. (3):

$$\Omega_p = \frac{\theta - \theta_{\text{birth}}}{t}, \quad (12)$$

where θ is the current position of the star, θ_{birth} is the position angle corresponding to the birthplace of the star, and t is the age of the star. In Table 2 this method is designated as “ $\theta - \theta_{\text{birth}}$ ”.

Following Dias and Lépine (2005), this Ω_{p} estimation method is called the direct one. It is applied in those cases where the space velocities of stars, their individual ages, and the membership in a specific spiral arm are known. Of course, the case in point are young stars affected by the spiral density wave. To determine the birthplaces of stars θ_{birth} , one usually constructs their Galactic orbits in the past using an appropriate model of the Galactic gravitational potential.

Using the direct method of analysis as applied to a sample of young OSCs, Naoz and Shaviv (2007) found $\Omega_p = 20.0^{+1.7}_{-1.2}$ km s⁻¹ kpc⁻¹ for the Perseus arm and $\Omega_p = 28.9^{+1.3}_{-1.2}$ km s⁻¹ kpc⁻¹ for the Local Arm. For two Carina-Sagittarius arms segments these authors found two values: $\Omega_{p1} = 16.5^{+1.2}_{-1.4}$ km s⁻¹ kpc⁻¹ and $\Omega_{p2} = 29.8^{+0.6}_{-1.3}$ km s⁻¹ kpc⁻¹.

Dias et al. (2019) analyzed the kinematics of ~ 440 OSCs younger than 50 Myr belonging to the Perseus, Local, and Carina-Sagittarius spiral arm segments. Data from the Gaia DR2 catalogue were used to calculate the average distances and proper motions of the clusters. Based on the direct method, with the determination of the OSC birthplace, the pattern speed and the corotation radius were estimated to be $\Omega_p = 28.2 \pm 2.1$ km s⁻¹ kpc⁻¹ and $R_{\text{cor}} = 8.51 \pm 0.64$ kpc, respectively. For the adopted $R_0 = 8.3$ kpc and $V_0 = 240$ km s⁻¹ the corotation radius here is $R_{\text{cor}} = (1.02 \pm 0.07)R_0$.

Based on various publications, Joshi and Malhotra (2023) produced a sample of 6133 OSCs most of which were detected already from Gaia data. Having analyzed the spatial distribution of these clusters, these authors showed that most of the OSCs left the spiral arms approximately 10–20 Myr after their formation. Having compared the current positions of ~ 440 young OSCs with their positions at birth, Joshi and Malhotra (2023) found $\Omega_p = 26.5 \pm 1.5$ km s⁻¹ kpc⁻¹ based on relation (13). These authors estimated the corotation radius ($R_{\text{cor}}/R_0 = 1.08^{+0.06}_{-0.05}$) by tying to the Galactic rotation curve specified by the potential from Bovy (2015), where $\Omega_0 = 27.5$ km s⁻¹ kpc⁻¹ ($V_0 = 220$ km s⁻¹ and $R_0 = 8.0$ kpc). Note that these authors considered a more complex version of Eq. (1) describing each spiral arm segment in the form of a sector structure:

$$R = R_{\text{kink}} e^{(\theta - \theta_{\text{kink}}) \tan i}, \quad (13)$$

where R_{kink} and θ_{kink} are the characteristics of the sector structure of the spiral arm.

Relative Methods

Below we will describe the results obtained by several methods. We call them relative, since they directly depend on the adopted angular velocity of Galactic rotation Ω_0 . In Table 2 the method based on the application of relations (6)–(9) is designated as “ ν ”.

When considering the relative shifts in the positions of stars caused by the spiral density wave in a time interval Δt , Eq. (3) will be written as

$$\ln\left(\frac{R}{R_0}\right) = \tan i \left[\theta - \theta_0 + \frac{\chi - \chi_0}{m} + (\Omega - \Omega_p) \Delta t \right], \quad (14)$$

At $R = R_0$ and $\theta = \theta_0 = 0$ we will have the following relation:

$$\Delta\Omega = \frac{\Delta\chi \times 10^3}{m\Delta t}, \quad (15)$$

Table 2: Ω_p estimated by various authors from young objects

Ω_p , km s ⁻¹ kpc ⁻¹	Objects	Method	Reference
11 – 13.5	OB stars	$\theta - \theta_{\text{birth}}$	(1)
~ 20	OB stars	ν	(2)
17.8 ± 3.1	OB stars	ν	(3)
19.1 ± 3.6	A,F,G supergiants and Cepheids	ν	(4)
21.3	OSC	$\theta - \theta_{\text{birth}}$	(5)
28.1 ± 2.0	Cepheids	ν	(6)
20 ± 2	OSC	$\theta - \theta_{\text{birth}}$	(7)
~ 30	OB stars	ν	(8)
24 ± 1	OSC	$\theta - \theta_{\text{birth}}$	(9)
18.6 ^{+0.3} _{-0.2}	~200 000 RAVE stars	ν	(10)
20.3 ± 0.5	OB stars	$\theta - \theta_{\text{birth}}$	(11)
23.0 ± 0.5	OSCs and giants	$\theta - \theta_{\text{birth}}$	(12)
25.2 ± 0.5	Cepheids	$\Delta\chi$	(13)
28.2 ± 2.1	OSC	$\theta - \theta_{\text{birth}}$	(14)
32.0 ± 0.9	OSC	$\theta - \theta_{\text{birth}}$	(15)
27 ± 1	Cepheids	$\Delta\chi$	(16)
26.5 ± 1.5	OSC	$\theta - \theta_{\text{birth}}$	(17)

(1) Lin et al. (1969); (2) Crézé and Mennessier (1973); (3) Byl and Ovenden (1978); (4) Mishurov et al. (1979); (5) Loktin and Matkin (1992); (6) Mishurov et al. (1997); (7) Amaral and Lépine (1997); (8) Fernández et al. (2001); (9) Dias and Lépine (2005); (10) Siebert et al. (2012); (11) Silva and Napiwotzki (2013); (12) Junqueira et al. (2015); (13) Dambis et al. (2015); (14) Dias et al. (2019); (15) Castro-Ginard et al. (2021); (16) Bobylev and Bajkova (2022e); (17) Joshi and Malhotra (2023).

where the phase difference $\Delta\chi$ is in radians, the age difference Δt is in Myr, and $\Delta\Omega = \Omega_0 - \Omega_p$ is in km s⁻¹ kpc⁻¹. In Table 2 this method is designated as “ $\Delta\chi$ ”.

Analysis of the Stellar Positions

Having analyzed the spatial positions of OSCs with various ages, Loktin and Matkin (1992) estimated $\Omega_p = 21.3$ km s⁻¹ kpc⁻¹. From the spatial distribution of classical Cepheids Dambis et al. (2015) found $\Omega_p = 25.2 \pm 0.5$ km s⁻¹ kpc⁻¹ averaged over three spiral arm segments.

By studying the distribution of Cepheids with various ages in the Carina-Sagittarius and Outer arms, Bobylev and Bajkova (2022d) estimated $\Omega_p = 27 \pm 1$ km s⁻¹ kpc⁻¹ and the corotation radius $R_{\text{cor}} = 9.0 \pm 0.3$ kpc ($R_{\text{cor}}/R_0 = 1.1 \pm 0.04$).

Analysis of the Stellar Kinematics

First note the results of applying relations (6)–(9). For example, Crézé and Mennessier (1973) found $\Omega_p = 20.0 \pm 4.1$ km s⁻¹ kpc⁻¹ from a sample of OB3 stars with the adopted $R_0 = 8$ kpc. Based on the kinematics of 183 AFG supergiants and a sample of 192 classical Cepheids, Mishurov et al. (1979) estimated $\Omega_p = 19.1 \pm 3.6$ km s⁻¹ kpc⁻¹. Later, based on

the kinematics of classical Cepheids, Mishurov et al. (1997) found $\Omega_p = 28.1 \pm 2.0 \text{ km s}^{-1} \text{ kpc}^{-1}$. Fernández et al. (2001) used this approach to study the kinematics of OB stars from the Hipparcos catalogue (1997) and obtained Ω_p close to $30 \text{ km s}^{-1} \text{ kpc}^{-1}$.

Lépine et al. (2001) applied this approach to justify the model consisting of a superposition of two- and four-armed spiral patterns. In particular, based on a sample of classical Cepheids with proper motions and line-of-sight velocities, they found $\Omega_p - \Omega_0 = 0.15$ and $0.18 \text{ km s}^{-1} \text{ kpc}^{-1}$ for the two- and four-armed spiral patterns, respectively. Thus, in this model the Sun is virtually at the corotation radius, with the corotation circle being slightly closer to the Galactic center than the Sun. This follows from the fact that the difference $\Omega_p - \Omega_0$ was found to be positive.

A positive difference $\Omega_p - \Omega_0 \approx 0.5 \text{ km s}^{-1} \text{ kpc}^{-1}$ was also obtained, for example, by Mishurov and Zenina (1999). These authors analyzed a sample of classical Cepheids with proper motions from Hipparcos (1997) and line-of-sight velocities and found $\Omega_0 = 27.3 \pm 1.7 \text{ km s}^{-1} \text{ kpc}^{-1}$ for $R_0 = 7.5 \pm 0.1 \text{ kpc}$. As a result, they concluded that the Sun is close to the corotation circle, since the difference $R_{\text{cor}} - R_0$ was $\approx 0.1 \text{ kpc}$.

In many of the cases listed in Table 2, where Ω_p was estimated by applying the Ω_p method, the difference $\Omega_p - \Omega_0$ is negative and, therefore, $R_{\text{cor}} > R_0$.

Based on 213 713 stars from the RAVE catalogue (Steinmetz et al. 2006), Siebert et al. (2012) estimated $\Omega_p = 18.6_{-0.2}^{+0.3} \text{ km s}^{-1} \text{ kpc}^{-1}$ for $m = 2$ using relations (6)–(9). Note that these authors also analyzed the four-armed model of the spiral structure ($m = 4$) and found $\Omega_p = 25.8_{-0.1}^{+0.1} \text{ km s}^{-1} \text{ kpc}^{-1}$.

The approach based on relation (16) is also applied. For example, Bobylev and Bajkova (2012) traced the change in radial phase $\Delta\chi$ obtained through a spectral analysis of the residual Cepheid velocities. As a result, from three samples of classical Cepheids with various ages, they found $\Omega_0 - \Omega_p = 10 \pm 3 \text{ km s}^{-1} \text{ kpc}^{-1}$ for the adopted $m = 2$ (then, $\Omega_0 - \Omega_p = 5 \pm 2 \text{ km s}^{-1} \text{ kpc}^{-1}$ for $m = 4$). Thus, taking $\Omega_0 = 29 \text{ km s}^{-1} \text{ kpc}^{-1}$ for Cepheids, we estimate $\Omega_p = 24 \pm 2 \text{ km s}^{-1} \text{ kpc}^{-1}$ for $m = 4$, which is in good agreement with the results in Table 1.

CONCLUSIONS

In this paper we used the estimates of the amplitudes of the velocity perturbations f_R and f_θ caused by the influence of a spiral density wave that were obtained by us previously from various stellar samples. These included: (i) Galactic masers with measured VLBI trigonometric parallaxes and proper motions, (ii) OB2 stars, and (iii) Cepheids. The proper motions of the OB2 stars and Cepheids were taken from the Gaia EDR3 catalogue.

The distances to the masers used were measured with errors less than 10%. The errors in the distances to the OB2 stars that were calculated based on their trigonometric parallaxes from the Gaia EDR3 catalogue have the same level. The distances to the Cepheids were calculated by Skowron et al. (2019) based on the period-luminosity relation with errors less than 5%. For all three samples the velocity perturbations f_R and f_θ were found using a spectral analysis.

From these data we obtained new estimates of the spiral pattern speed Ω_p : 24.61 ± 2.06 , 24.71 ± 1.29 and $25.98 \pm 1.37 \text{ km s}^{-1} \text{ kpc}^{-1}$ from the samples of masers, OB2 stars, and Cepheids, respectively. The corotation radii R_{cor}/R_0 for these three samples are 1.16 ± 0.09 , 1.15 ± 0.06 and 1.09 ± 0.06 , suggesting that corotation is close to the Sun, with the corotation

circle being located between the Sun and the Perseus arm segment.

The results obtained by us from these three samples are in excellent agreement between themselves. However, the Ω_p estimates obtained by other authors in recent years lie in a fairly wide range of $\Omega_p : 18 - 32 \text{ km s}^{-1} \text{ kpc}^{-1}$.

ACKNOWLEDGMENTS

We are grateful to the referee for the useful remarks that contributed to an improvement of the paper.

REFERENCES

1. I. A. Acharova, J. R. D. Lépine, Yu. N. Mishurov, B.M. Shustov, A. V. Tutukov, and D. S. Wiebe, *Mon. Not. R. Astron. Soc.* 402, 1149 (2010).
2. L. H. Amaral and J. R. D. Lépine, *Mon. Not. R. Astron. Soc.* 286, 885 (1997).
3. R. I. Anderson, H. Saio, S. Ekström, C. Georgy, and G. Meynet, *Astron. Astrophys.* 591, A8 (2016).
4. R. A. Benjamin, E. Churchwell, B. L. Babler, L. Brian, T. M. Bania, D. P. Clemens, M. Cohen, J. M. Dickey, et al., *Publ. Astron. Soc. Pacif.* 115, 953 (2003).
5. V. V. Bobylev and A. T. Bajkova, *Astron. Lett.* 38, 638 (2012).
6. V. V. Bobylev and A. T. Bajkova, *Mon. Not. R. Astron. Soc.* 437, 1549 (2014).
7. V. V. Bobylev and A. T. Bajkova, *Astron. Rep.* 65, 498 (2021).
8. V. V. Bobylev and A. T. Bajkova, *Astron. Rep.* 66, 269 (2022) a.
9. V. V. Bobylev and A. T. Bajkova, *Astron. Lett.* 48, 376 (2022) b.
10. V. V. Bobylev and A. T. Bajkova, *Astron. Lett.* 48, 169 (2022) c.
11. V. V. Bobylev, A. T. Bajkova, *Astron. Rep.* 66, 545 (2022) d.
12. V. V. Bobylev and A. T. Bajkova, *Astron. Lett.* 48, 568 (2022) e.
13. J. Bovy, *Astrophys. J. Suppl. Ser.* 216, 29 (2015).
14. J. Byl and M. W. Ovenden, *Astrophys. J.* 225, 496 (1978).
15. A. Castro-Ginard, P. J. McMillan, X. Luri, et al., *Astron. Astrophys.* 652, 162 (2021).
16. D. Chakrabarty, *Astron. Astrophys.* 467, 145 (2007).
17. X. Chen, S.Wang, L. Deng, R. de Grijs, and M. Yang, *Astrophys. J. Suppl. Ser.* 237, 28 (2018).
18. M. Crézé and M. O. Mennessier, *Astron. Astrophys.* 27, 281 (1973).
19. A. K. Dambis, L. N. Berdnikov, Yu. N. Efremov, A. et al., *Astron. Lett.* 41, 489 (2015).
20. W. S. Dias and J. R. D. Lépine, *Astrophys. J.* 629, 825 (2005).
21. W. S. Dias, H. Monteiro, J. R. D. Lépine, and D. A. Barros, *Mon. Not. R. Astron. Soc.* 486, 5726 (2019).
22. A.-C. Eilers, D. W. Hogg, H.-W. Rix, et al., *Astrophys. J.* 900, 186 (2020).
23. D. Fernández, F. Figueras, and J. Torra, *Astron. Astrophys.* 372, 833 (2001).
24. O. Gerhard, *Mem. Soc. Astron. It. Suppl.* 18, 185 (2011).
25. E. Griv, L.-G. Hou, I.-G. Jiang, and C.-C. Ngeow, *Mon. Not. R. Astron. Soc.* 464, 4495 (2017).
26. The HIPPARCOS and Tycho Catalogues, ESA SP-1200 (1997).
27. T. Hirota, T. Nagayama, M. Honma, Y. Adachi, R. A. Burns, J. O. Chibueze, Y. K. Choi, K. Hachisuka, et al. (VERA Collab.), *Publ. Astron. Soc. Jpn.* 70, 51 (2020).
28. Y. C. Joshi and S. Malhotra, arXiv: 2212.09384 (2023).
29. T. C. Junqueira, C. Chiappini, J. R. D. Lépine, et al., *Mon. Not. R. Astron. Soc.* 449, 2336 (2015).
30. J. R. D. Lépine, Yu. N. Mishurov, and S. Yu. Dedikov, *Astrophys. J.* 546, 234 (2001).

31. C. C. Lin and F. H. Shu, *Astrophys. J.* 140, 646 (1964).
32. C. C. Lin, C. Yuan, and F. H. Shu, *Astrophys. J.* 155, 721 (1969).
33. A. V. Loktin and N. V. Matkin, *Astron. Astrophys. Trans.* 3, 169 (1992).
34. L. S. Marochnik, Yu. N. Mishurov, and A. A. Suchkov, *Astrophys. Space Sci.* 19, 285 (1972).
35. L. S. Marochnik and A. A. Suchkov, *Astrophys. Space Sci.* 79, 337 (1981).
36. M. Martos, X. Hernandez, M. Yáñez, E. Moreno, and B. Pichardo, *Mon. Not. R. Astron. Soc.* 350, L47 (2004).
37. T. A. Michtchenko, J. R. D. Lépine, A. Pérez-Villegas, R. S. S. Vieira, and D. A. Barros, *Astrophys. J. Lett.* 863, L37 (2018).
38. Yu. N. Mishurov, E. D. Pavlovskaya, and A. A. Suchkov, *Astron. Rep.* 56, 268 (1979).
39. Yu. N. Mishurov, I. A. Zenina, A. K. Dambis, A. M. Mel'nik, and A. S. Rastorguev, *Astron. Astrophys.* 323, 775 (1997).
40. Yu. N. Mishurov and I. A. Zenina, *Astron. Astrophys.* 341, 781 (1999).
41. Yu. N. Mishurov and I. A. Acharova, *Mon. Not. R. Astron. Soc.* 412, 1771 (2011).
42. S. Naoz and N. J. Shaviv, *New Astron.* 12, 410 (2007).
43. J. Palouš, J. Ruprecht, O. B. Dluhnevskaya, and T. Piskunov, *Astron. Astrophys.* 61, 27 (1977).
44. J. Palouš, *Astron. Astrophys.* 87, 361 (1980).
45. B. Pichardo, M. Martos, E. Moreno, and J. Espresate, *Astrophys. J.* 582, 230 (2003).
46. A. C. Quillen and I. Minchev, *Astron. J.* 130, 576 (2005).
47. A. S. Rastorguev, E. V. Glushkova, M. V. Zabolotskikh, and H. Baumgardt, *Astron. Astrophys. Trans.* 20, 103 (2001).
48. M. J. Reid, K. M. Menten, A. Brunthaler, X.W. Zheng, T.M. Dame, Y. Xu, Y. Wu, B. Zhang, et al., *Astrophys. J.* 783, 130 (2014).
49. M. J. Reid, K. M. Menten, A. Brunthaler, X.W. Zheng, T.M. Dame, Y. Xu, J. Li, N. Sakai, et al., *Astrophys. J.* 885, 131 (2019).
50. K. Rohlfs, *Lectures on Density Wave Theory* (Springer, Berlin, 1977).
51. A. Siebert, B. Famaey, J. Binney, et al., *Mon. Not. R. Astron. Soc.* 425, 2335 (2012).
52. M. D. V. Silva and R. Napiwotzki, *Mon. Not. R. Astron. Soc.* 431, 502 (2013).
53. D. M. Skowron, J. Skowron, P. Mróz, A. Udalski, et al., *Science* (Washington, DC, U. S.) 365, 478 (2019).
54. M. Steinmetz, T. Zwitter, A. Siebert, F. G. Watson, et al., *Astron. J.* 132, 1645 (2006).
55. A. Udalski, M. K. Szymański, and G. Szymański, *Acta Astron.* 65, 1 (2015).
56. J. P. Vallée, *Astrophys. J.* 454, 119 (1995).
57. J. P. Vallée, *Astrophys. J.* 566, 261 (2002).
58. J. P. Vallée, *Astron. J.* 135, 1301 (2008).
59. J. P. Vallée, *New Astron. Rev.* 79, 49 (2017a).
60. J. P. Vallée, *Astrophys. Space Sci.* 362, 79 (2017b).
61. J. P. Vallée, *Mon. Not. R. Astron. Soc.* 506, 523 (2021).
62. S. Wang, X. Chen, R. de Grijs, and L. Deng, *Astrophys. J.* 852, 78 (2018).
63. Y. Xu, L. G. Hou, S. Bian, et al., *Astron. Astrophys.* 645, L8 (2021).
64. C. Yuan, *Astrophys. J.* 158, 889 (1969).